Study of the Characterization and Curing of Benzoxazines using ^{13}C Solid-State Nuclear Magnetic Resonance

VERNON M. RUSSELL, JACK L. KOENIG, HONG YEE LOW, H. ISHIDA

Department of Macromolecular Science, Case Western Reserve University, Cleveland, Ohio 44106-7202

Received 2 September 1997; accepted 13 January 1998

ABSTRACT: Benzoxazines derived from bisphenol-A, formaldehyde, and primary amines were characterized using ^{13}C solid-state NMR spectroscopy. The two 1,3-benzoxazines studied in this work are 2,2′-(3-methyl-4-dihydro-1,3,2-benzoxazine)propane, (**B-m**) and 2,2′-(3-phenyl-4-dihydro-1,3,2-benzoxazine)propane (**B-a**). Solid-state ^{13}C-NMR spectra were obtained for **B-m** and **B-a** and the observed peak positions were noted. These resonances agreed well with chemical shifts calculated based on the chemical structure. Samples of **B-m** and **B-a** were cured at two different temperatures: 150 and 200°C. The polymerizations induced spectral changes including new resonances, intensity changes, and line-width broadenings. Kinetic analysis of the curing data gave different kinetic parameters for the two cure temperatures, which is expected since the first cure temperature is below the material's glass transition temperature (T_g) while the second cure temperature is above the T_g. © 1998 John Wiley & Sons, Inc. J Appl Polym Sci 70: 1413–1425, 1998

Key words: benzoxazines; NMR; curing; branching

INTRODUCTION

Synthetic polymers have played an ever-increasing role in modern-day life. These materials show up in almost every aspect of scientific, industrial, and household applications. In 1910, phenolic resins became the first synthetic polymers to be mass produced.[1] Since then, phenolic resins have played an important role in the plastics industry. Their associated properties including excellent insulating characteristics and thermal properties made them ideal to replace the more expensive and rare natural resins such as shellac and *gutta percha*. Further, the lightweight and processing flexibility of these resins allowed manufacturers to incorporate new designs into their products.

Benzoxazines are a specific class of phenolic resin materials. They are heterocyclic structures consisting of a benzene ring fused with an oxazine ring (a six-membered ring that includes one oxygen atom and one nitrogen atom). The properties of benzoxazines are typical for phenolic resins. They exhibit good heat resistance and flame retardance and have good dielectric properties. Some benzoxazines have been found to display interesting pharmaceutical properties including anti-inflammatory and central nervous system depressing agents[2] and antibacterial activity against *Staphylococcus aureus* and *Escherichia coli*.[3]

There has been an ongoing effort to develop new chemistry and processing techniques for benzoxazines[4] which may generate new forms of this compound for use in modern markets such as in the electronics and aerospace industries. Two of these compounds, which are 3,4-dihydro-3-substituted-1,3-benzoxazines, were the primary focus of this research.

A common synthetic pathway for the generation of benzoxazines involves the reaction of phe-

Correspondence to: J. L. Koenig.

Journal of Applied Polymer Science, Vol. 70, 1413–1425 (1998)
 CCC 0021-8995/98/071413-13

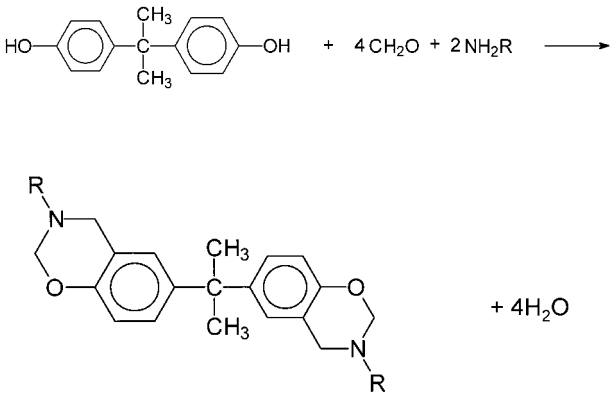

Figure 1 Synthesis of **B-m** and **B-a.**

nol, amine, and aldehyde. It has been found that this synthetic pathway can be modeled as a Mannich-type reaction.[5,6] The synthesis reaction of 2,2′-(3-methyl-4-dihydro-1,3,2-benzoxazine)propane (**B-m**) and 2,2′-(3-phenyl-4-dihydro-1,3,2-benzoxazine)propane (**B-a**) are shown in Figure 1. The benzoxazine ring (containing the O and N atoms) is the reactive site for curing of the benzoxazine. Benzoxazines may be monofunctional or difunctional. The latter case may produce crosslinked structures.

Solid-state NMR

Solid-state NMR has been used to study phenolic resins[7,8] as well as benzoxazines.[9] Further, there have been substantial chemical-shift assignments observed for benzoxazine.[10–12] Techniques including cross polarization (CP), dipolar decoupling (DD), and magic angle spinning (MAS) are used to obtain ^{13}C-NMR spectra in the solid state. Spinning at the magic angle of 54.7° is necessary to reduce the chemical-shift anisotropy (CSA) broadening which is due to geometric-dependent magnetic interactions. This leaves only the isotropic chemical shift.[13] Cross polarization increases the intensity of ^{13}C resonances by transferring magnetization from the abundant proton-spin reservoir to the dilute carbon-spin reservoir. It is also beneficial to use cross polarization for ^{13}C solid-state NMR spectroscopy because its low natural abundance (1.1%) and low sensitivity are often insufficient for practical spectral acquisition times. The advantages of cross polarization for observing ^{13}C signals are twofold. First, the ^{13}C observed signal is up to four times more intense (the ratio between the gyromagnetic ratios of ^{1}H and ^{13}C, respectively. Second, it is possible to use shorter recycle delays[14] since the spin-lattice relaxation times of ^{1}H nuclei are much shorter than those of ^{13}C nuclei. Dipolar decoupling is necessary to reduce the line broadening arising from heteronuclear dipolar couplings between ^{1}H and ^{13}C nuclei.[15]

Curing Studies

The curing of polymers has been studied using ^{13}C-NMR spectroscopy.[16,17] Since ^{13}C chemical shifts are sensitive to local environments, changes in the environment will yield a change in the chemical shift of a particular atom. Thus, the presence of molecular species during a curing process may be followed by ^{13}C-NMR. Using the identifications of those resonances native to the monomer structure and those native to the polymer structure, it is possible to quantify changes in the structure of the material. Further, it has been shown that the identification of intermediate species during the curing process is possible using NMR.[16,17] In this manner, the nature of the chemical reaction upon curing can be examined.

Crosslinking

The ^{13}C solid-state NMR spectrum is dependent on many factors. Some of these have been discussed earlier and relate to general nuclear interactions and relaxations. However, changes in a sample undergoing polymerization not only yield changes in the peak intensity and chemical shifts, but may also cause changes for resonances of those nuclei which are not directly involved in the polymerization process. An example of this is the peak line width for a carbon whose chemical environment is not chemically affected by the curing of the material. The line broadening of such a peak may be used to follow polymerization effects such as mobility changes and crosslinking.

The line width of an NMR peak is dependent on CSA, dipolar coupling, T_2 (spin–spin relaxation time), field inhomogeneity, and other less contributing factors. There have been studies examining the correlation between line width and chemical crosslink density.[17] The two factors which

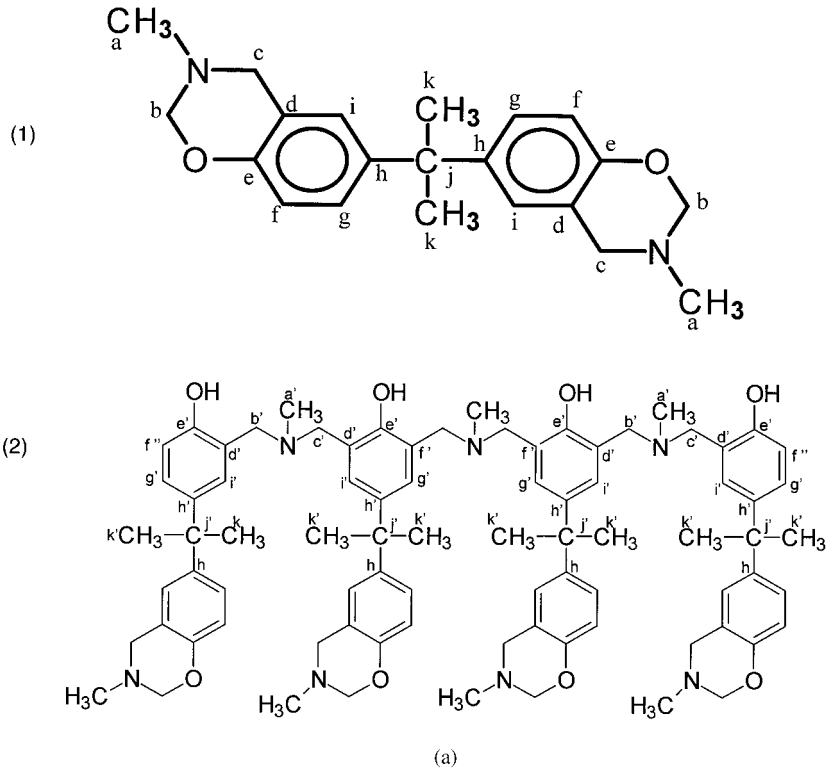

Figure 2 (a) Chemical structure of **B-m** monomer and **B-m** tetramer.

contribute to line broadening with increased crosslinking density are relaxation effects and chemical-shift effects. If the mobility of atoms within the sample decreases with crosslinking, the increased restriction results in changes in relaxation times and may contribute to changes in line width.

Benzoxazine Curing

The polymer structure of the benzoxazines used in this research are significantly different from that of the monomers, that is, the breaking of the benzoxazine ring upon curing results in the formation of Mannich bridge structures and phenol substituents. Since these are major structural changes, it should be possible to observe changes in the ^{13}C-NMR spectrum as polymerization proceeds.

The curing processes of phenolic resins have been studied thoroughly by NMR,[16] differential scanning calorimetry (DSC),[18] and isothermal DSC experiments.[19] The kinetics of the polymerization reaction can be studied if several assumptions are made: First, we write the rate of reaction ($d\alpha/dt$) for this system as given by the general self-catalyzed reaction function:

$$\dot{\alpha} = \frac{d\alpha}{dt} = k(1 - \alpha)^n \alpha^m$$

where α is the degree of conversion, k is the kinetic constant, and m and n are the kinetic exponents. It has been shown that these benzoxazines undergo an autocatalytic ring-opening reaction.[19,20] Further, if we assume an overall reaction order of two, which has also been observed for these benzoxazines,[19,20] then we arrive at the formula

$$\ln\left(\frac{\dot{\alpha}}{\alpha^2}\right) = \ln k + n \ln\left(\frac{1 - \alpha}{\alpha}\right)$$

EXPERIMENTAL

Labeled structures of the monomer and polymer of **B-m** and **B-a** are shown in Figure 2(a) and (b), respectively. Figure 3 shows possible crosslinks in the **B-m** benzoxazine system. Chemical shifts were

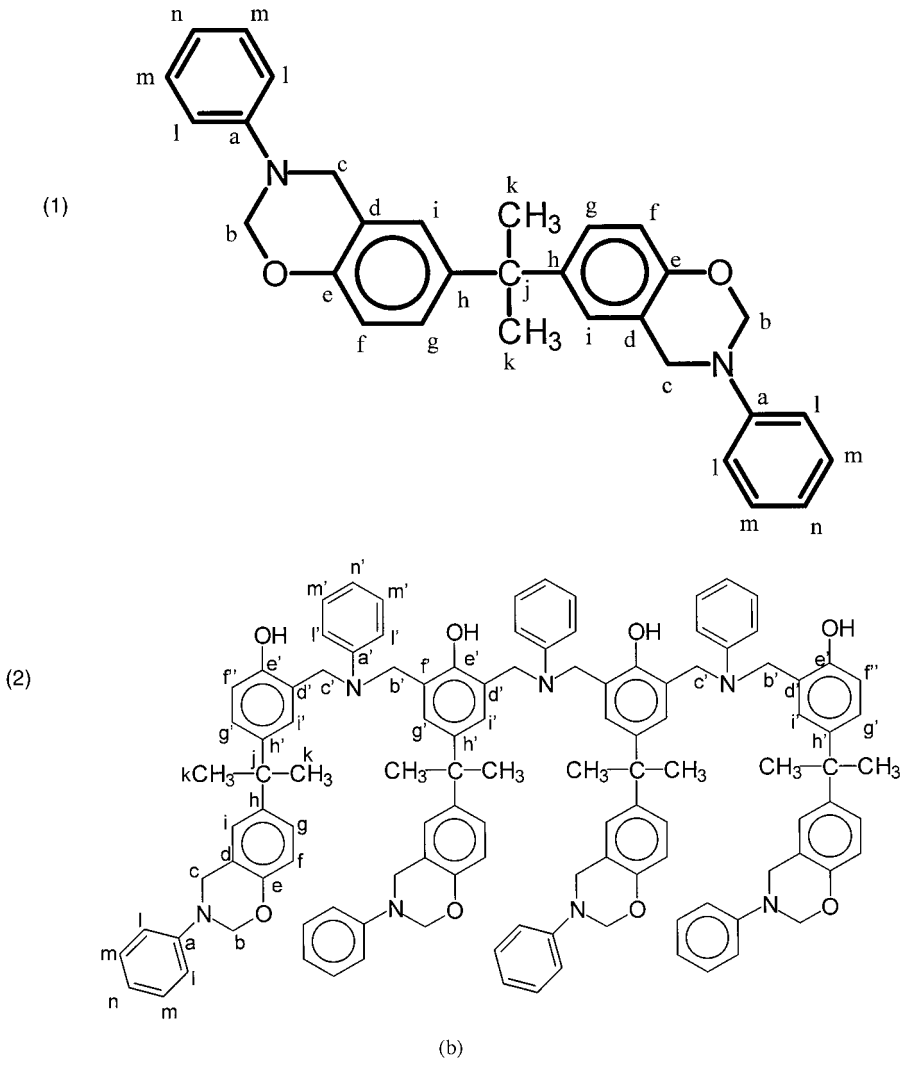

Figure 2 (*Continued from the previous page*) (b) Chemical structure of **B-a** monomer and **B-a** tetramer.

calculated using substituent additivity tables and reference compounds. The calculated chemical shifts for both the monomer and polymer structures are given in Table I(a) and (b) for **B-m** and **B-a,** respectively. All NMR experiments were performed on a Bruker MSL-300 spectrometer at a ^{13}C spectra frequency of 75.47 MHz. Variable contact time cross-polarization experiments were conducted to determine the optimum contact time. An example of the variable contact time curve is shown in Figure 4 for the quaternary resonance of **B-m** (carbon j at 41 ppm). This contact time (800 μs) was used for all experiments thereafter. The CP–MAS–DD spectrum of **B-m** is shown in Figure 5 at spinning speeds of 3, 4, and 5 kHz. For these spectra, 2000 scans were accumulated before Fourier transformation. The recycle delay for each cross-polarization experiment was 2 s. The CP–MAS–DD spectra of **B-m** and **B-a** are compared in Figure 6. The DD–MAS spectrum was obtained using a recycle delay of 15 s and an MAS speed of 4 kHz. This spectrum was very similar to the CP–MAS–DD spectrum but took a considerably longer time to acquire. This illustrated the advantages of using cross polarization for the reduction of the acquisition time. The TOSS (total suppression of spinning side bands) spectra of **B-m** and **B-a** were collected using delays set for total side-band elimination and were useful in the determination of spinning side bands.

B-m and **B-a** were cured at two different temperatures: 150 and 200°C. CP-MAS spectra were obtained at various stages in the polymerization

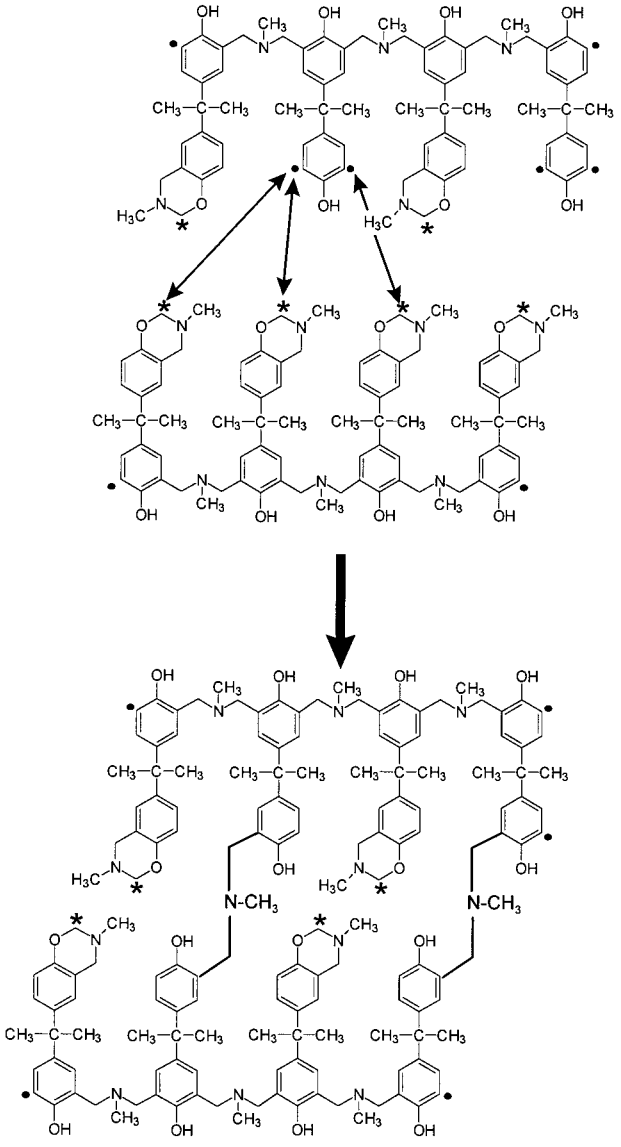

Figure 3 Structure showing possible crosslinks between two **B-m** polymer molecules.

process. Two thousand transients were accumulated for the curing spectra using the CP–MAS–DD techniques. Contact times of 800 μs and recycle delays of 2 s were used for all curing spectra.

RESULTS

Representative spectra taken during the polymerization process of **B-m** at 150°C are shown in Figure 7. It was found that the ^{13}C peak at 152 ppm decreased in intensity during cure. Conversely, a peak appeared at 157 ppm and increased in intensity during polymerization. This is illustrated in Figure 8(a) which is 3D representation of the 162–136 ppm spectra region. From left to right, we see one peak (157 ppm) increase with cure time, one peak (152 ppm) decrease with cure time, and a third peak (142 ppm) remain constant with cure time. The peak at 152 ppm is assigned to the aromatic carbon bonded to the oxygen atom of the oxazine ring and is character-

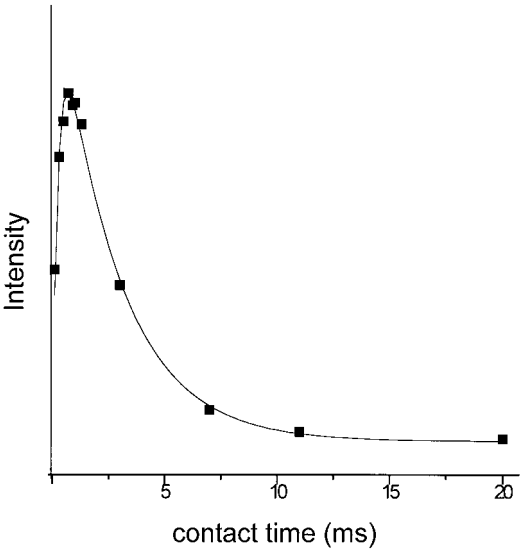

Figure 4 Variable contact cross-polarization curve for the quaternary resonance of **B-m** (carbon j at 41 ppm).

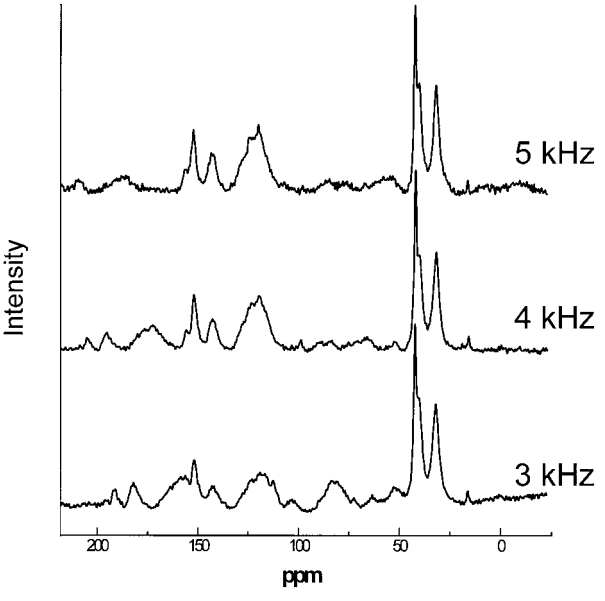

Figure 5 CP-MAS spectra of MBA at 3, 4, and 5 kHz.

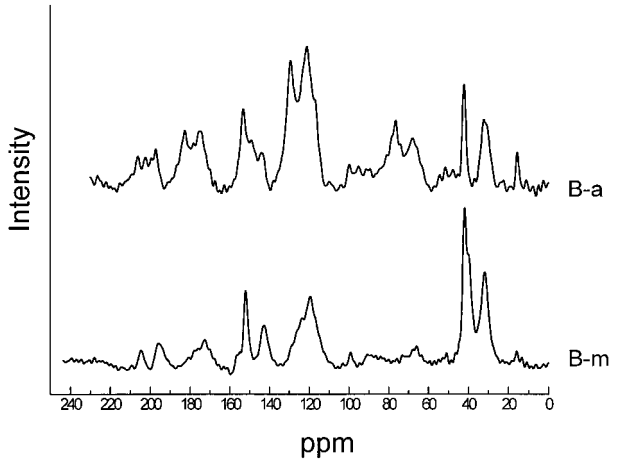

Figure 6 CP-MAS spectra of **B-m** and **B-a.**

istic of the monomer [carbon e in Fig. 2(a) (1)]. The peak at 157 is assigned to carbon e′ of the **B-m** polymer [Fig. 2(a) (2)] and is formed as the benzoxazine ring opens. The third peak, at 142 ppm, is assigned to the aromatic carbon bonded to the quaternary carbon [carbon h and h′ for Fig. 2

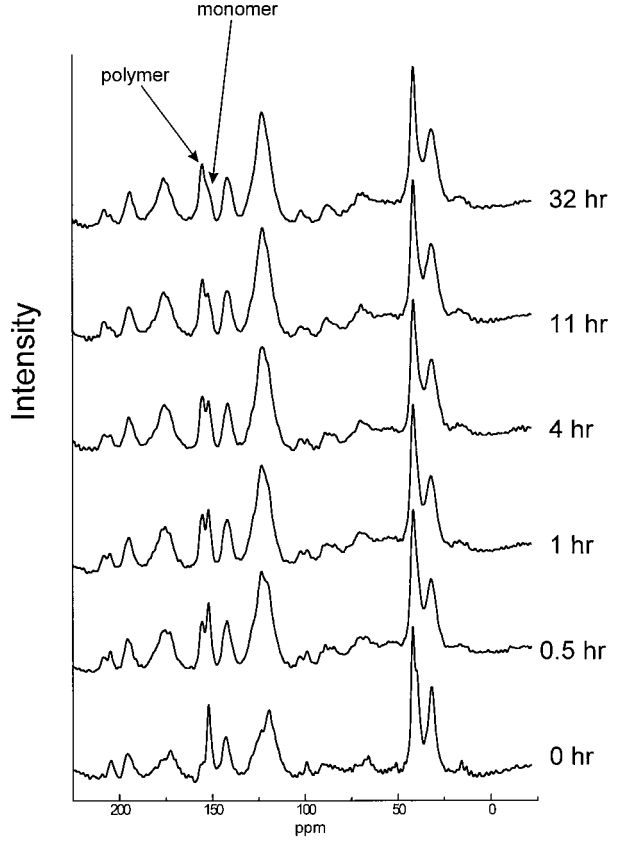

Figure 7 Spectra of **B-m** during cure at 150°C.

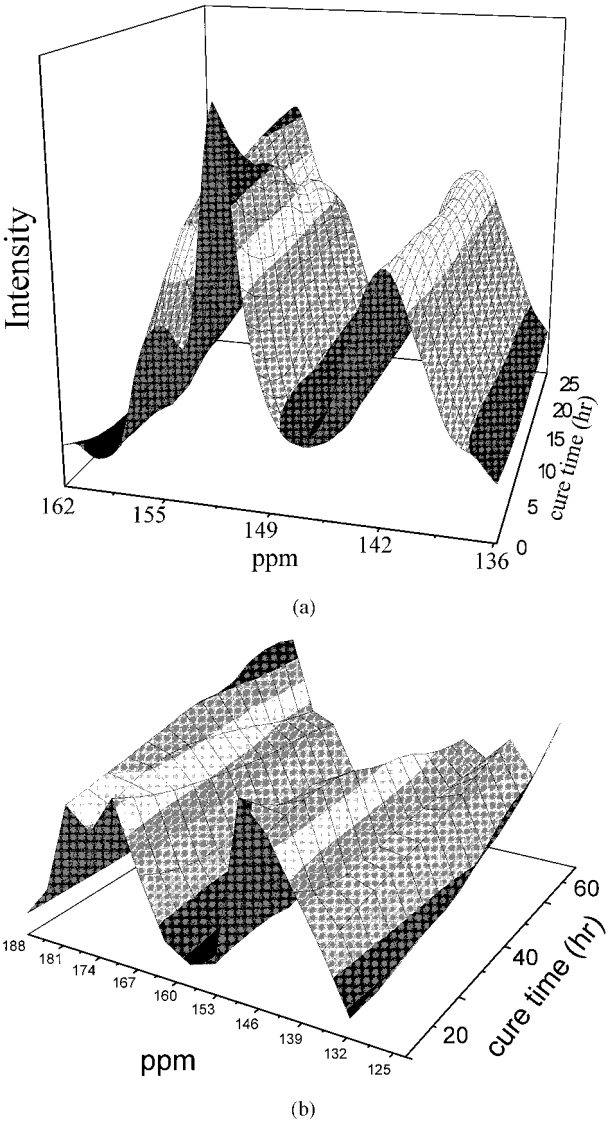

Figure 8 (a) 3D representation of peak changes during curing of **B-m** at 150°C. (b) 3D representation of peak changes during curing of **B-a** at 150°C.

(1) and (2)] and does not change upon polymerization. Another peak was formed during the later stages of the polymerization of **B-m** at 200°C and is present in the spectra shown in Figure 9 for the cure times over 11 h. This peak (at 119 ppm) is assigned to an aromatic carbon of a degradation product which is formed during extended exposure to elevated temperatures.

During the cure of **B-a,** it was observed that the ^{13}C peaks at 151 and 148 ppm decreased in intensity during cure. This is illustrated in Figure 8(b), which is a 3D representation of the 188–125 ppm spectral region and shows the plotted inten-

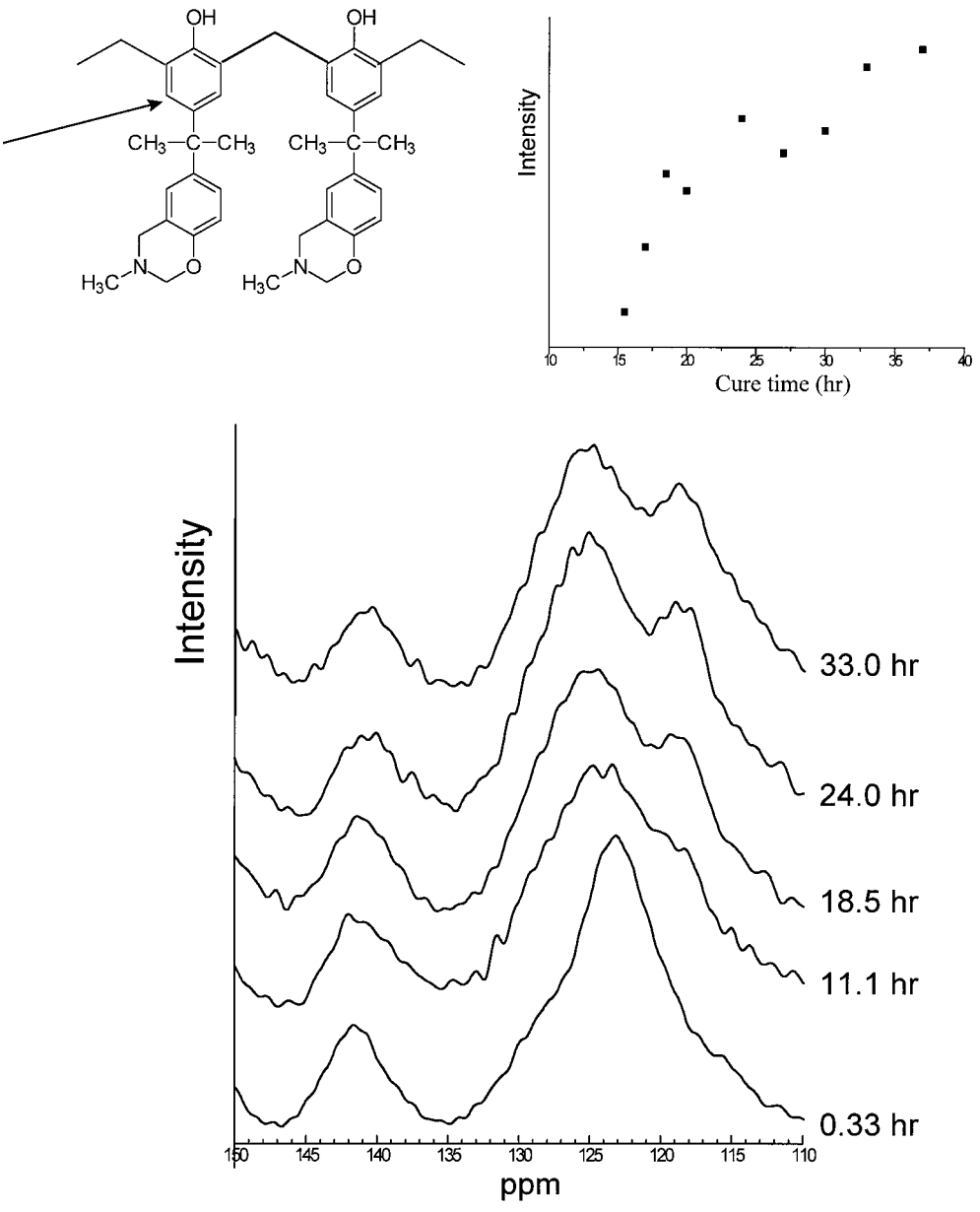

Figure 9 Changes in peak intensity of a new **B-m** resonance formed during latter stages of cure at 200°C.

sity versus cure time. The peak at 151 ppm is assigned to the aromatic carbon bonded to the oxygen atom of the oxazine ring [carbon e in Fig. 2(b) (1)] and is characteristic of the **B-a** monomer. As in the case of **B-m,** the later stages of polymerization of **B-a** at 200°C yielded a resonance at 120 ppm which is assigned to the corresponding degradation product of **B-a.**

The change in peak intensity for the 152 ppm resonance of **B-m** at 150°C is shown in Figure 10. Estimates of the uncertainties in peak intensity were calculated by taking two spectra of identical cure times, such that the first spectrum was taken immediately upon removal of the sample from the oven while the second spectrum was taken after the sample was left overnight without additional cure. Plots of peak area versus cure time were also constructed for the peaks mentioned earlier, but no significant changes from the intensity plots were observed. Finally, it was observed that a peak around 16 ppm was present in the majority of the monomer samples of both **B-m**

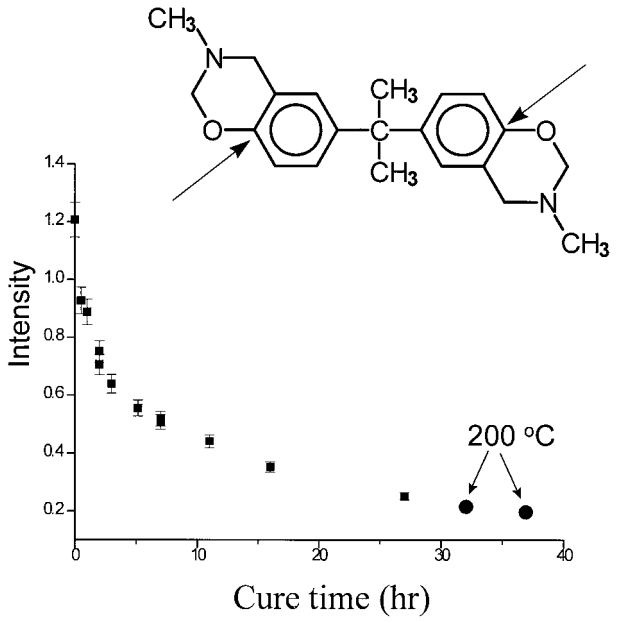

Figure 10 Changes in peak intensity for the 152 ppm peak at 150°C.

and **B-a,** and upon cure, this peak usually increased in intensity. There is no chemical-shift assignment for this peak based on the benzoxazine structures discussed so far. However, this resonance could be assigned to a substituted ethylamine and is assumed to be due to an impurity.

Since the intensity of an NMR peak is proportional to the number of those structures present, it is possible to estimate the relative concentration of a structure present during the polymerization process. Further, it is possible to estimate the extent of reaction, α, by the following formula

$$\alpha = 1 - \frac{I_t}{I_0}$$

where I_t is the intensity of a monomer peak at time t and I_0 is the intensity of the monomer peak at time $t = 0$ (no cure). The plots of α versus cure time for **B-m** and **B-a** are shown in Figure 11(a) and (b), respectively during polymerization at 150°C. The assumption of overall second-order kinetics was made and examples of the resultant logarithmic plots are shown in Figure 12(a) and (b) for **B-m** and **B-a,** respectively.

A line-width study was conducted on the curing spectra of **B-m** and **B-a** at both cure temperatures. It was found that line width of the methyl peak (31 ppm) increased during the polymerization for both materials at both cure temperatures. This is shown in Figure 13(a,b). The line widths of other carbons were also studied and are shown in Figure 14 (aromatic carbon of **B-m**) and Figure 15 (quaternary carbon of **B-a**).

DISCUSSION

The calculated chemical shifts of the benzoxazine monomers showed good agreement with the observed chemical shifts [shown in Table I(a,b)], proving that the proposed monomer structures[4] were indeed present. The calculated chemical shifts of the polymeric structures also show good

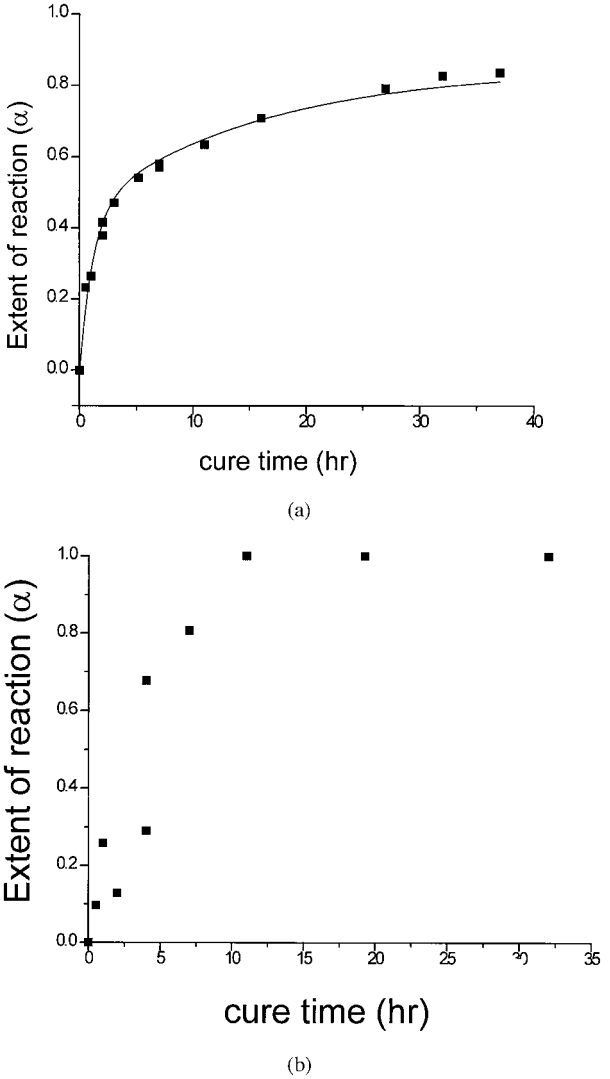

Figure 11 (a) Extent of reaction (α) of **B-m** versus cure time at 150°C. (b) Extent of reaction (α) of **B-a** versus cure time at 150°C.

agreement with the observed chemical shifts of the polymers. Further, most chemical shifts exclusive to the monomer are weak or absent in the polymer spectrum, whereas most chemical shifts native to the polymer are weak or absent in the monomer spectrum. Figure 3 shows some of the possible crosslinks that can occur between two **B-m** polymer chains. The chemical shifts for the crosslinking structures are very similar to those of the polymer and thus direct evidence of crosslinking is not available from the chemical-shift data.

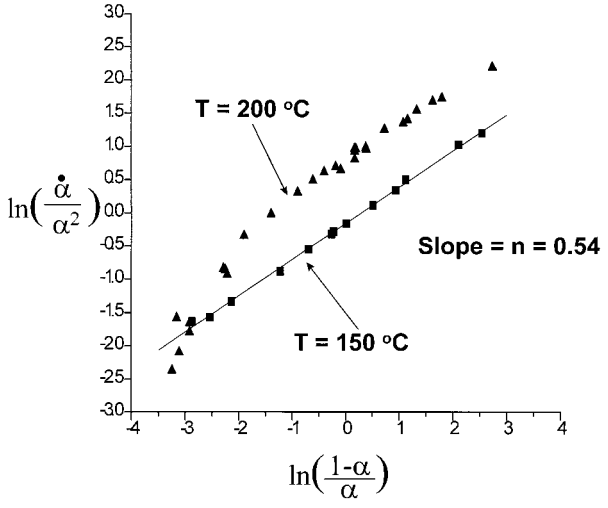

(a)

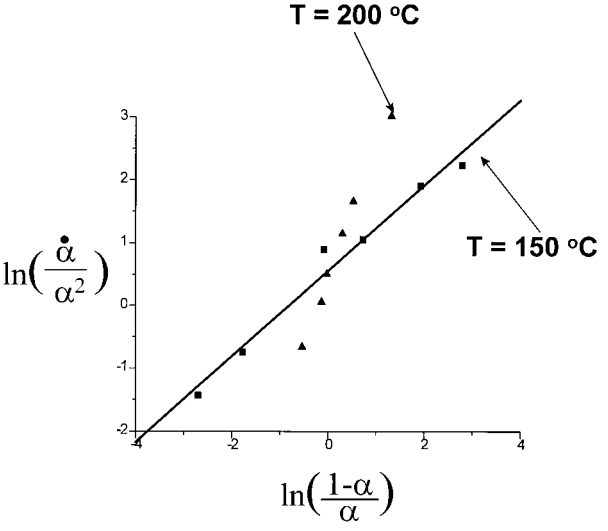

(b)

Figure 12 (a) Kinetic plot of **B-m** at 150 and 200°C assuming overall reaction order of 2. (b) Kinetic plot of **B-a** at 150 and 200°C assuming overall reaction order of 2.

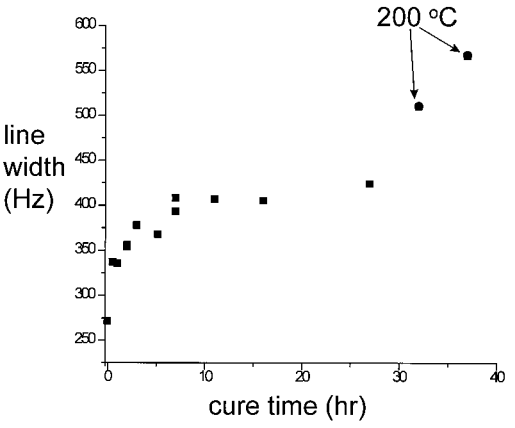

(a)

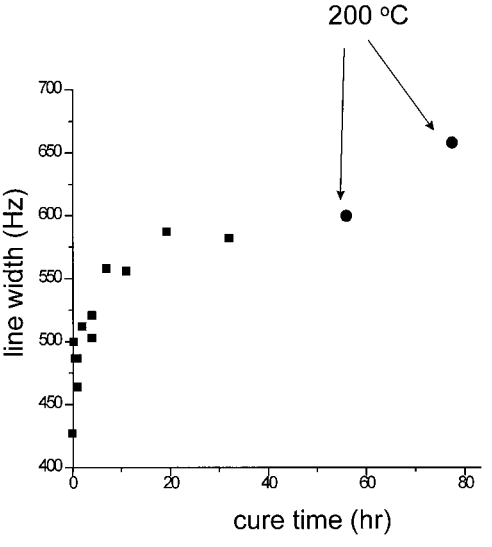

(b)

Figure 13 (a) Plot of **B-m** NMR line width versus cure time for aliphatic peak at 31 ppm at cure temperature of 150°C. (b) Plot of **B-a** NMR line width versus cure time for aliphatic peak at 31 ppm at cure temperature of 150°C.

The plots of intensity changes versus cure time for **B-m** exhibited opposite trends for the 152 and 157 ppm peaks. These resonances were selected for the polymerization study. The logarithmic plots of $\ln(\alpha/\alpha^2)$ versus $\ln[(1 - \alpha)/\alpha]$ in Figure 12(a,b) gave excellent linear fits for the first cure temperature with slope n equal to 0.54 for **B-m** and 0.67 for **B-a** at 150°C. The logarithmic plots for the second cure temperature showed a different behavior. While an initial slope of 0.59 was observed for the **B-m** benzoxazine, the final slope of 1.3 was detected. This indicates that there are different mechanisms in the curing process at 200°C as compared to 150°C. The slope of the

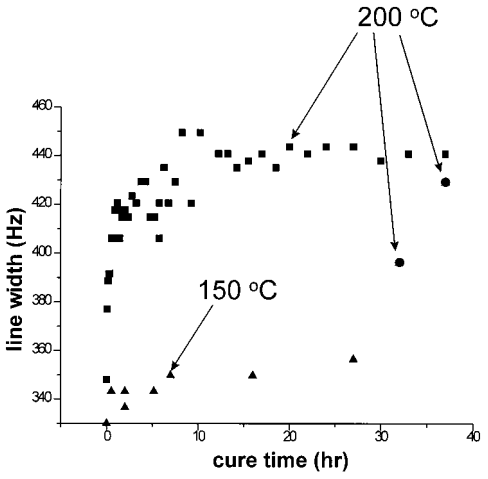

Figure 14 Plot of **B-m** NMR line width versus cure time for aromatic peak at 142 ppm at 150 and 200°C.

kinetic curve of **B-a** at 200°C was approximately 2 during the later stages of the cure. Thus, a similar behavior exists for these benzoxazines in that both compounds show linear fits during cure at 150°C, but shown nonlinearity for polymerization at 200°C.

Benzoxazines of this type have been shown to undergo a cationic polymerization.[20,21] It has been shown that the ring-opening initiation of this kind of benzoxazine results in the formation of a carbocation and an iminium ion in equilibrium[21] (see Fig. 16). In this case, the stability of the iminium ion greatly affects the propagation rate since it is the carbocation that was proposed to be the species responsible for propagation.[21] Further, the basicity of the amine group used greatly affects the reactivity of the equilibrium pair. The more basic the amine, the more the free electron pair of the nitrogen will be able to stabilize the positive charge of the iminium ion. If the iminium ion is stable, the equilibrium is shifted toward it, resulting in a state of low propagation. However, if the iminium ion is unstable, the equilibrium will be shifted toward the carbocation, resulting in a higher propagation rate.

It should be noted that temperature does have a great impact on the rate of propagation which is expected since the propagation reaction involves chain transfer to a benzene ring. This type of reaction is highly dependent on temperature.[22] Thus, for the early stages of polymerization, the reaction may be relatively independent of the cure temperature. As the reaction proceeds, the temperature effect on propagation would become more evident in the reaction kinetics.

The other main difference between the curing experiments at the different temperatures is that one curing experiment was conducted below the glass transition temperature (T_g) and the other was conducted above the T_g for both compounds. It has been shown that a higher cure temperature results in a vitrification state sooner than a lower cure temperature, especially when below the T_g of these materials.[23] Vitrification is accompanied by a large increase in the viscosity of the system at which time the reaction becomes largely diffusion-controlled, which will greatly affect the curing kinetics.

Referring to Figure 13(a,b), after a sharp initial increase in the line width of the methyl carbon (31 ppm), the rate of increase levels off around 20-h cure time for both benzoxazines. However, to ensure full polymerization, the curing temperature was then increased to 200°C and cured for an additional 17 h. During the additional cure at this increased temperature, a further increase in line width was observed for this aliphatic peak. This trend is observed for other carbons as well for the first cure experiment. The increase in line width for the aromatic carbon (carbon h at 142 ppm) of **B-m** is shown in Figure 14 at 150 and 200°C. The trends shown here are similar to the results from the other carbons discussed.

The line-width broadenings observed for **B-a** were similar to those discussed for **B-m.** However, in the case of **B-a,** the quaternary carbon (carbon j at 41 ppm) was used since for this polymer there is no overlapping methyl amine resonance. The broadening trend of this resonance is shown in Figure 15 at both cure temperatures.

The source of the observed line broadening, as mentioned earlier, can be due to either relaxation

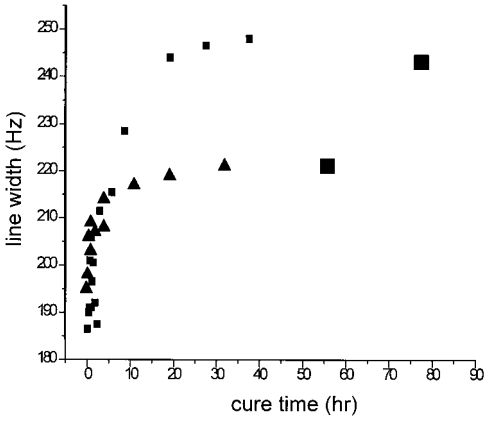

Figure 15 Plot of **B-a** NMR line width versus cure time for quaternary peak at 41 ppm at 150 and 200°C.

Table I Chemical Shifts for (a) B-m Monomer and Polymer and (b) B-a Monomer and Polymer

Carbon	Calculation	Value	Observed Monomer	Observed Polymer
		(a)		
a	−2.3 + 42	39.7	40s	—
a′	−2.3 + 42	39.7	40s	—
b	−2.3 + 42 + 58 − 5.3	92.4	91m	—
b′	−2.3 + 43 + 23	62.7	64m	62w
c	−2.3 + 42 + 23 − 5.3	57.4	56m	—
c′	−2.3 + 42 + 23	62.7	62m	62w
d	128.5 + 15.6 − 14.4 − 0.4	129.3	128m	126s
d′	128.5 + 15.6 − 12.7 − 0.4	131	—	126s
e	128.5 + 31.4 − 0.5 − 3.1	156.3	152s	152w
e′	Reference	157	157w	157s
f	128.5 − 14.4 − 0.4	113.7	115w	—
f′	128.5 − 12.7 + 0 + 0	115.8	115w	119s
g	128.5 − 2.6 + 1.0 − 3.4	123.5	124m	126s
g′	128.5 + −2.0 + 1.6 + −2.5	125.6	124m	126s
h	128.5 + 22.2 − 7.7	143.0	142s	142s
h′	128.5 + 22.2 + 7.7	143.0	142s	142s
i	128.5 − 2.0 + 1.0 − 3.4	124.1	124m	126s
i′	128.5 − 2.0 + 1.0 − 3.4	124.1	124m	126s
j	Reference	41	42s	42s
j′	Reference	41	42s	42s
k	Reference	31	31s	31s
k′	Reference	31	31s	31s
		(b)		
a	128.5 + 22.4	150.9	148.5ms	—
a′	128.5 + 22.4	150.9	148ms	151s
b	−2.3 + 42 + 58	97.7	97mw	—
b′	−2.3 + 43 + 23	62.7	64m	61w
c	−2.3 + 42 + 23	62.7	65mw	—
c′	−2.3 + 42 + 23	62.7	64m	61w
d	128.5 + 15.6 − 14.4 − 0.4	129.3	128s	128s
d′	128.5 + 15.6 − 12.7 − 0.4	131	128s	128s
e	128.5 + 31.4 − 0.5 − 3.1	156.3	152s	—
e′	Reference	157	—	156s
f	128.5 − 14.4 − 0.4	113.7	117m	111w
f′	128.5 − 12.7 + 15.6 − 0.4	131	128	128s
g	128.5 − 2.6 + 1.0 − 3.4	123.5	121s	128s
g′	128.5 + 1.6 − 2.6 − 3.4	124.1	—	126s
h	128.5 + 22.2 − 7.7	143.0	143ms	142s
h′	128.5 + 22.2 − 7.3	143.4	143s	142s
i	128.5 − 2.0 + 1.0 − 3.4	124.1	128s	128s
i′	128.5 − + 1.6 − 0.5 − 3.4	126.2	—	126s
j	Reference	41	41s	41s
j′	Reference	41	41s	41s
k	Reference	31	31s	31s
k′	Reference	31	31s	31s
l	128.5 − 15.7	112.8	117m	119s
l′	128.5 − 15.7	112.8	117m	119s
m	128.5 + 0.8	129.3	129s	128s
m′	128.5 + 0.8	129.3	129s	128s
n	128.4 − 11.8	116.7	117m	119s
n′	128.5 − 11.8	116.7	117m	119s

Relative peak intensities are given by w (weak), m (medium), or s (strong).

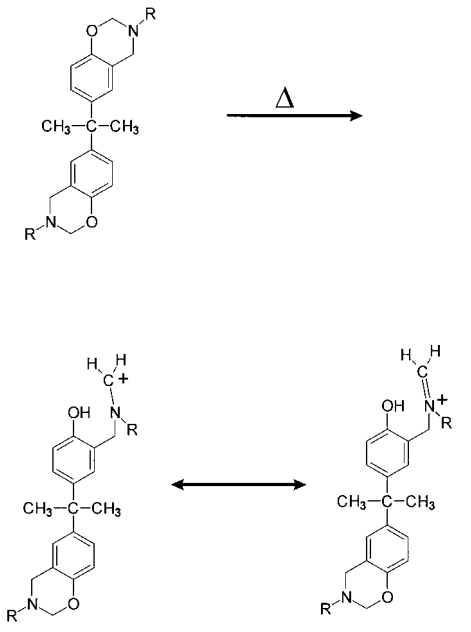

Figure 16 Ring-opening reaction of benzoxazine.

effects or chemical-shift dispersion effects. The former has already been discussed and we will assume that the latter is the major source for line broadening. The secondary increases in line width in the latter stages of cure can be explained two ways: First, it is possible that the sample was not fully polymerized at the initial leveling off stage and that exposure to the higher temperature continued to cure the sample. Second, it is possible that the increase in temperature resulted in the production of crosslinked structures since this would increase the chemical-shift dispersion of the resonances in the spectra. The changes in line width for other peaks were also studied (Figs. 14 and 15) for the aromatic and quaternary carbons, respectively. These figures show a similar trend for the first cure temperature in that the line width constantly increases with cure time up to a leveling-off point and then increases further upon increasing the temperature to 200°C. However, for the second cure study, the line width increases steadily with time and levels off with no further increase. The line width of the methyl peak is often always a good indicator for the entire structure since the motion of a methyl group may be largely independent of the group motions of the backbone chain. However, in this case, the line broadening displayed by the methyl peak shows a similar trend compared to other resonances studied.

A spin-lattice relaxation study (T_1) was performed on the monomers and polymers. It was found that resonances from the monomer exhibited single exponential decays, whereas resonances from the polymer exhibited more than one exponential decay. This is expected due to the variation in molecular environments present in the polymer. Of the polymer T_1 analysis, the short relaxation times agreed well with the monomer relaxation times. This result is expected since the monomer structure is relatively the same for all molecules present. However, the polymer molecules consist of a variety of different structures which would result in a distribution of relaxation times.

CONCLUSION

The 3,4-dihydro-3-substituted-1,3-benzoxazines, **B-m** and **B-a,** were characterized using ^{13}C solid-state NMR spectroscopy. There was good agreement between the observed and calculated chemical shifts for both the monomer and polymer structures. The results from the cure studies indicate that the reaction kinetics are significantly different for the two cure temperatures of 150 and 200°C. The polymerization is influenced by several factors including the nature of cationic polymerization kinetics, the difference of the temperatures with respect to the glass transition temperature, and the temperature dependence of the propagation reaction. It was also observed that the line width of the methyl peak at 31 ppm as well as other resonances change significantly during the curing process even though those carbons' immediate environment do not change significantly. This broadening occurs due to increases in degree of polymerization as well as to increases in the crosslink density.

REFERENCES

1. D. I. Whitehouse, J. Pritchett, and J. Barnett, in *Phenolic Resins,* ILIFFE, London, 1967.
2. B. D. Tilak, N. R. Ayyangar, and U. S. Rao, *Indian J. Chem. B,* **23,** 18 (1984).
3. M. F. El-Zohry, A. N. Ahmed, F. A. Omar, and A. M. Abd-Alla, *J. Chem. Technol. Biotechnol.,* **53,** 329 (1992).
4. X. Ning and H. Ishida, *J. Polym. Sci. Part A Polym. Chem.,* **32,** 1121 (1994).
5. F. W. Holly and A. C. Cope, *J. Am. Chem. Soc.,* **66,** 1875 (1944).
6. W. J. Burke, E. L. M. Glennie, and C. Weatherbee, *J. Org. Chem.,* **29,** 909 (1964).

7. R. L. Bryson, G. R. Hatfield, T. A. Early, A. R. Palmer, and C. E. I. Macie, *Macromolecules,* **16,** 1669 (1983).
8. P. Sohar, G. Bernath, S. Frimpong-Manso, A. E. Szabo, and G. Stajer, *Magn. Reson. Chem.,* **28,** 1045 (1990).
9. K. Neuvonen and K. Pihlaja, *Magn. Reson. Chem.,* **28,** 239 (1990).
10. K. V. Prasad Rao, P. S. N. Reddy, and V. Sundaramurthy, *Magn. Reson. Chem.,* **24,** 644 (1986).
11. K. Neuvonen, R. Pohtola, and K. Pihalja, *Magn. Reson. Chem.,* **27,** 725 (1989).
12. K. Neuvonen and K. Pihlaja, *ACTA Chem. Scand.,* **47,** 695 (1993).
13. E. R. Andrew, *Philos. Trans. R. Soc. Lond. A,* **299,** 505 (1981).
14. M. H. Levitt, D. Suter, and R. R. Ernst, *J. Chem. Phys.,* **84,** 4243 (1986).
15. J. L. Koenig, *Spectroscopy of Polymers,* American Chemical Society, Washington, DC, 1992.
16. G. R. Hatfield and G. E. Maciel, *Macromolecules,* **20,** 608 (1987).
17. P. W. Kopf and E. R. Wagner, *J. Polym. Sci. Polym. Chem. Ed.,* **11,** 939 (1973).
18. H. Ishida and Y. Rodriguez, *Polymer,* **36,** 3151 (1995).
19. J. Jang and S. Shin, *Polym. J.,* **27,** 601 (1995).
20. S. B. Shen, *Ph.D. thesis,* Case Western Reserve University, Cleveland, OH, 1995.
21. J. Albuquerque Cid, *Ph.D. thesis,* Case Western Reserve University, Cleveland, OH, 1996.
22. P. J. Flory, *Principles of Polymer Chemistry,* Cornell University Press, Ithaca, NY, 1953.
23. Y. Rodriguez, *M.S. thesis,* Case Western Reserve University, Cleveland, OH, 1993.